Atmos. Chem. Phys., 7, 315–327, 2007
www.atmos-chem-phys.net/7/315/2007/

Atmospheric Chemistry and Physics

Two-years of NO_3 radical observations in the boundary layer over the Eastern Mediterranean

M. Vrekoussis[1,*], N. Mihalopoulos[1], E. Gerasopoulos[1,], M. Kanakidou[1], P. J. Crutzen[2], and J. Lelieveld[2]**

[1]Environmental Chemical Processes Laboratory, Department of Chemistry, University of Crete, P.O. Box 2208, 71003 Voutes, Heraklion, Greece
[2]Max-Planck-Institut für Chemie, Abt. Luftchemie, Mainz, Germany
[*]now at: Institute of Environmental Physics and Remote Sensing IUP/IFE, University of Bremen, Bremen, Germany
[**]now at: Institute of Environmental Research and Sustainable Development, National Observatory of Athens, Athens, Greece

Received: 29 June 2006 – Published in Atmos. Chem. Phys. Discuss.: 28 September 2006
Revised: 12 January 2007 – Accepted: 12 January 2007 – Published: 22 January 2007

Abstract. This is the first study that investigates the seasonal variability of nitrate (NO_3) radicals in the marine boundary layer over the East Mediterranean Sea. An extensive data set of NO_3 radical observations on the north coast of Crete for more than two years (June 2001–September 2003) is presented here. NO_3 radicals follow a distinct seasonal dependency with the highest seasonally average mixing ratios in summer (5.6±1.2 pptv) and the lowest in winter (1.2±1.2 pptv). Episodes with high NO_3 mixing ratios have been encountered mainly in polluted air masses originating from mainland Greece, Central and East Europe, and Turkey. Ancillary measurements of ozone, nitrogen dioxide (NO_2) and meteorological parameters have been conducted and used to reveal possible relationship with the observed NO_3 variability. The acquired NO_2 nighttime observations provide the up-to-date most complete overview of NO_2 temporal variability in the area. The data show correlations of the NO_3 nighttime mixing ratios with temperature (positive), relative humidity (negative) and to a lesser extend with O_3 (positive). As inferred from these observations, on average the major sink of NO_3 radicals in the area is the heterogeneous reaction of dinitrogen pentoxide (N_2O_5) on aqueous particles whereas the homogeneous gas phase reactions of NO_3 are most important during spring and summer. These observations support a significant contribution of NO_3 nighttime chemistry to the oxidizing capacity of the troposphere.

Correspondence to: M. Kanakidou
(mariak@chemistry.uoc.gr)

1 Introduction

The self-cleaning efficiency of the troposphere is important for air quality, and depends on the oxidation and deposition of trace constituents. The most important oxidants in the atmosphere are the hydroxyl radical (OH) during daytime, the nitrate radical (NO_3) during nighttime, and ozone (O_3) during the entire day.

In the presence of nitrogen dioxide (NO_2) and ozone (O_3), NO_3 radicals are formed in the lower troposphere mainly via Reaction (R1):

$$NO_2 + O_3 \rightarrow NO_3 + O_2 \quad \text{(R1)}$$

During daytime NO_3 radicals do not build up to measurable levels (ca. 1 pptv) because they have a short lifetime of about 5 s (Orlando et al., 1993) due to the radiation absorption in the visible band of the solar spectrum (maximum absorption at 662 nm) and consequent photodissociation to NO_2 and to a lesser extent NO (Reaction R2b).

$$NO_3 + h\nu \rightarrow NO_2 + O(^3P), \quad \lambda_1 < 580\,\text{nm} \quad \text{(R2a)}$$

$$NO_3 + h\nu \rightarrow NO + O_2, \quad \lambda_2 < 700\,\text{nm} \quad \text{(R2b)}$$

NO_3 radicals also react rapidly in the gas phase with NO to form NO_2. In polluted areas this reaction might dominate the sink of NO_3 during daytime. At night, NO levels are low, especially in areas far from primary NO_x emissions. This in addition to the absence of light, which dissociates NO_3 radicals, allows the build up of significant NO_3 mixing ratios during night.

Besides its role in the formation of NO_3 radicals, NO_2 also acts as a transient sink for NO_3 to form N_2O_5 via the

Published by Copernicus GmbH on behalf of the European Geosciences Union.

temperature dependant equilibrium (R3,−3) (Atkinson et al., 2004):

$$NO_3 + NO_2 + M \leftrightharpoons N_2O_5 + M \quad \text{(R3,−3)}$$

The equilibrium (R3,−3) depends strongly on temperature and therefore N_2O_5 can act as a reservoir or as a sink for nitrate radicals and subsequently the nitrogen oxides (NO_x=NO+NO_2) depending on ambient temperature. Gas-phase N_2O_5 might contribute to nitric acid formation via reaction with water vapor, a process that is probably slow though uncertain (Wahner et al., 1998; Atkinson et al., 2003). Most importantly, N_2O_5 undergoes heterogeneous reactions with water on aerosol or/and in clouds to form HNO_3 and nitrate (NO_3^-) anions, thus leading to a net loss of NO_3 and NO_x. Reported uptake coefficients of N_2O_5 (the ratio of the number of gas molecules removed by the condensed phase divided by the number of gas molecules colliding with the particle) γ_{N2O5} on different aerosol surfaces vary from 2×10^{-4} to 0.04 depending on temperature and surface composition with the lowest values observed for aerosols containing organics (Schutze at al., 2002; Zetsch et al., 1992; Hu and Abbatt, 1997; Badger et al., 2006; Brown et al., 2006).

The direct hydrolysis of NO_3 radicals is slow with γ_{NO3} equal 4.4×10^{-4} at 273 K (Rudich et al., 1996) In the aqueous phase NO_3 can also react with anions like Cl^- to produce NO_3^- anions with $\gamma_{NO3}\geq2\times10^{-3}$ at 293 K (Thomas et al., 1998).

The NO_3 radicals undergo gas phase reactions with Volatile Organic Compounds (VOCs) (Atkinson, 2000) and form peroxy (RO_2) and hydroxyl (OH) radicals (e.g. Platt et al., 1990; Carslaw et al., 1997a, b; Salisbury et al., 2001). They also contribute to the conversion and subsequent removal of NO_x to reactive nitrogen (Allan et al., 1999) forming nitric acid (HNO_3) and particulate nitrate (NO_3^-) during night (Brown et al., 2004; Vrekoussis et al., 2006).

Although for most VOCs, the rates of reactions with NO_3 are lower than those with OH (Atkinson et al., 2004), there are several VOCs that are very reactive towards NO_3; for example, dimethylsulfide (DMS), isoprene, monoterpenes, some alkenes and some aromatics. NO_3 reactions with VOCs proceed either via H-abstraction, forming HNO_3 (e.g. with aldehydes, higher alkanes and DMS) or NO_3 addition, forming nitrated organic peroxides, which is the case of alkenes and other unsaturated VOCs. During night NO_3 mixing ratios can be 10–100 times higher than of hydroxyl radicals during the day. In these cases NO_3 radicals can be the main atmospheric oxidant for species with similar reactivity towards NO_3 and OH radicals (for instance various pinenes, Atkinson et al., 2004). Therefore, atmospheric processes driven by NO_3 radicals, involving both gas phase and heterogeneous chemistry, may be of importance for the oxidizing capacity of the atmosphere and for nutrient nitrate formation. To our knowledge only two studies have addressed the role of NO_3 on a seasonal basis (Heintz et al., 1996; Geyer et al., 2001a). Seasonal NO_3 radical measurements are challenging because of the low mixing ratios and high spatial and temporal variability involved.

The present study aims to investigate the seasonal variability of NO_3 radicals and the controlling factors in the marine planetary boundary layer over the East Mediterranean Sea. This region attracts attention as it is a cross point of various air masses of different origin. Depending on the wind direction, polluted air masses with important loading of NO_x and anthropogenic aerosol are alternate with cleaner air originating from the Atlantic Ocean and Sahara, e.g. with low O_3 and significant dust loading (Mihalopoulos et al., 1997; Kouvarakis et al., 2000; Lelieveld et al., 2002).

2 Location of the station and experimental setup

Nitrate radicals were measured by a long path differential optical absorption spectroscopy (DOAS) instrument (Platt and Perner, 1983) along a 10.4 km light beam at Finokalia station (35.3′ N, 25.3′ E) on the island of Crete in the East Mediterranean for more than two years (June 2001–September 2003). The sampling station characteristics and the experimental device used for NO_3 measurements have been described in detail elsewhere (Mihalopoulos et al., 1997; Kouvarakis et al., 2000; Vrekoussis et al., 2004). NO_3 radicals are detected via their two significant absorption bands at 623 and 662 nm in the visible region of the solar spectrum. To eliminate influences such as water bands, NO_2 and lamp structures, the corresponding reference spectra are fitted simultaneously to derive the NO_3 signal, as described by Martinez et al. (2000) and Vrekoussis et al. (2004). Finally, the optical density of NO_3 is quantified through the 662 nm peak using the absorption cross section reported by Yokelson et al. (1994). The integration time ranged from 10 to 30 min depending on the visibility through the light path. Note that a single measurement is the average of several individual absorption spectra over a long optical path in the atmosphere of 10.4 km, thus reducing the influence of small-scale variability. The detection limit (signal to noise ratio S/N=3) for the NO_3 radicals has been estimated to 1.2 pptv.

Nitrogen dioxide has been measured in parallel with NO_3 by changing the region of the light spectrum between the visible (VIS) for NO_3 and the ultraviolet (UV) region for NO_2 detection. NO_2 quantification has been achieved by using the optical density of the 405 nm peak and the cross section provided by Yoshino et al. (1997). Unfortunately, the NO_2 data set is not as extended as the NO_3 observations due to the increased noise in the UV region caused by a malfunction of the Photo Diode Arrays. Only good quality spectra (signal to noise ratio larger than 3) are used for the present analysis. The mean detection limit for NO_2 mixing ratios was 0.18 ± 0.04 ppbv.

Short path UV absorption instrument (Dasibi – 1008) has been used for the continuous 5-min O_3 measurements during these two years. The instrument has a detection limit equal

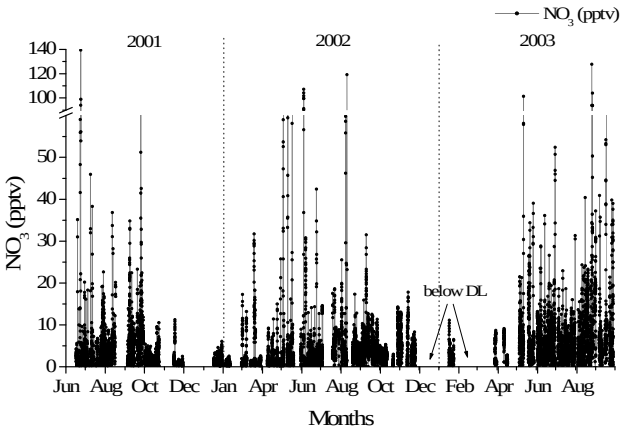

Fig. 1. NO_3 observations (in pptv) at Finokalia during 2 years of sampling (June 2001–September 2003).

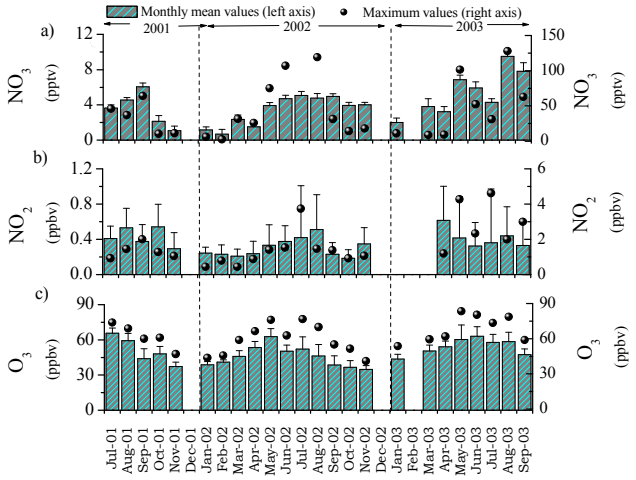

Fig. 2. Monthly mean mixing ratios (left axis) of **(a)** NO_3, **(b)** NO_2 and **(c)** O_3 and their standard deviations (nighttime observations only). Black squares, circles and triangles depict the maximum values per month (right axis) of NO_3, NO_2 and O_3, respectively.

to 1 ppbv as indicated by the manufacturer. An extensive 5-min O_3 record since 1997 has been reported and analysed by Kouvarakis et al. (2000, 2002) and Gerasopoulos et al. (2005, 2006). Nitrogen monoxide is experimentally determined by a Thermo Environmental Model 42C high sensitivity chemiluminescence NO_x analyzer equipped with a molybdenum converter that in addition to NO and NO_2, allows detection of PAN, nitric acid, and organic nitrates. The radioisotope Radon-222 has also been measured for this study with a 2-h sampling time and detection limit better than 1 mBq/m^3, and is used as a tracer of continental air masses (see details in Gerasopoulos et al., 2005). The meteorological parameters (temperature, relative humidity, wind speed and direction and solar irradiance) have been measured by an automated meteorological station and then averaged over 5 min intervals. Local time (LT) is used for the presentation and the discussion of the results hereafter.

3 Results and discussion

3.1 NO_3 variability and impact of transport

Measurements were performed during a total of 392 nights from June 2001 to September 2003. During 336 nights, NO_3 radical mixing ratios were above the detection limit of 1.2 pptv (Fig. 1) and in 8 cases exceeded 100 pptv. The maximum observed NO_3 value was 139 pptv (June 2001) and the nighttime monthly mean value of the 2-year period was 4.2±2.3 pptv (arithmetic average ± standard deviation).

As shown in Table 1, the monthly or seasonally averaged NO_3 observations compare fairly well with data reported earlier for various locations and similar time periods. However, the random peak levels of NO_3 observed at Finokalia mainly during summer exceed by 40% earlier reported maximum NO_3 values in the continental (100 pptv in autumn, Brown et al., 2003) and in the marine boundary layer (98 pptv in spring, Heintz et al., 1996) and are significantly lower than those recorded by Platt et al. (1980) in Riverside, California (up to 300 pptv). Our values are lower than those reported by Sebastian (2004) for Finokalia during July 2000, period during which the area has been affected by exceptionally high biomass burning events.

Since O_3 and NO_2 are precursors to NO_3 radical formation (R1), examination of their levels and variability is essential for understanding the chemistry of NO_3. Figures 2a–c show the monthly mean (and maximum) nighttime mixing ratios of NO_3 radicals, NO_2 and O_3, observed during the studied period. NO_3 radical levels are high in spring (seasonal average 3.7±0.9 pptv) and summer (5.6±1.2 pptv) and low during winter (1.2±1.2 pptv), and follow those of its precursors, NO_2 and O_3 and of NO_3lifetime depicted in Table 2 (see discussion in Sect. 3.3.2).

The NO_2 data series acquired with the DOAS instrument and presented here (Fig. 2b) provides the most complete overview of NO_2 temporal variability at a coastal area in the Eastern Mediterranean since only few NO_2 measurements have been reported in the literature for the area (Kourtidis et al., 2002; Vrekoussis et al., 2004). The individual NO_2 measurements range from below the detection limit (0.18 ppbv) up to 5 ppbv. The annual mean NO_2 mixing ratio based on observations above the detection limit is 0.31±0.13 ppbv. The lowest monthly average of 0.24 ppbv was observed in winter and the highest (about 0.60 ppbv) in spring and summer.

Similarly to NO_2 and NO_3, O_3 minimum levels were registered in winter (seasonal average value equals 37±6 ppbv) while the highest levels were observed in late spring–mid summer (summer seasonal average of 56±10 ppbv) (Fig. 2c). For the studied 2-year period, the annual mean mixing ratio

Table 1. NO_3 radical measurements for different environments and seasons reported in the literature. L: total path of the used DOAS instrument.

Location	Latitude-Longitude	NO_3 Average (pptv)	NO_3 Max (pptv)	L (km)	Time/Season	Year	Ref
			Continental Boundary Layer				
Lindenberg, Germany	52°13′ N–14°07′ E	4.6	85	10	Feb–Sep	1998	Geyer et al. (2001a)
		5.0	–	10	March–April	1998	“
		5.7	–	10	May–Sep	1998	“
Pabstthum, Germany	52°51′ N–12°56′ E	–	70	12.6	July–Aug	1998	“
Boulder, Colorando, U.S.	40°6 N–105°16 W	–	100	–	Oct–Nov	2001	Brown et al. (2003)
Riverside, California, U.S.	33°56′ N–117°23′ W	–	288	–	Sep	1979	Platt et al. (1980)
			Marine Boundary Layer				
Kap Arkona (Rügen Island), Germany	54°30′ N–13°30′ E	7.8	98	7.3	April 1993–May 1994	1993/94	Heintz et al. (1996)
Izana, Tenerife, Spain (2003 m)	28°40′ N–16°05′ W	8.0	20	9.6	May	1994	Carslaw et al. (1997a)
		–	20	9.3	June/July	1997	Allan et al. (2000)
Wayborne, England	52°57′ N–1°08′ E	9.7 SP*	–	5	Winter (4 nights)	1994	Allan et al. (1999)
		10.0	25	5	Spring (4 nights)	1994	Carslaw et al. (1997b)
		6 CL*	–	5	Summer (4 nights)	1995	Allan et al. (1999)
		11.1	–	5	Autumn (1 night)	1994	Carslaw et al. (1997b)
Mace Head, Ireland	53°19′ N–9°54′ W	1–5 CL* 1–40 SP*	40	8.4	July/August	1996	Allan et al. (2000)
		1–5 CL* 1–40 SP*	40	8.4	April/May	1997	idem
		3 CL* 13 SP*	25	8.4	July/August	2005	Saiz-Lopez et al. (2006)
Helgoland, island	54°2′ N–7°9′ E	P	40	3.6	October	1996	Martinez et al. (2000)
Finokalia, Greece	35°30′ N–25°7′ E	4.5	37	10.4	July/August	2001	Vrekoussis et al. (2004)
		20.8	307.7	8.2	July	2000	Sebastian (2004)
		5.6	139.3	10.4	Summer	2001	This work
		3.4	64.1	10.4	Autumn	2001	“
		1.0	6.0	10.4	Winter	2002	“
		2.9	75.2	10.4	Spring	2002	“
		5.3	119.2	10.4	Summer	2002	“
		4.7	31.5	10.4	Autumn	2002	“
		2.2	11.1	10.4	Winter	2003	“
		5.1	101.4	10.4	Spring	2003	“
		7.2	127.7	10.4	Summer	2003	“
		7.8	62.9	10.4	September	2003	“

* CL=Clean conditions; SP=Semi-polluted conditions; P=Polluted conditions

of O_3 is 48±9 ppbv with the 5-min observations ranging from 23 ppbv to 83 ppbv. Details on the seasonal variation of O_3 at Finokalia are given by Gerasopoulos et al. (2005).

The impact of the air mass origin on the levels of NO_3 radicals and other chemical species of interest for the present study has been investigated for the 2-year period. The rose diagrams shown in Figs. 3a–f have been constructed by averaging within each 10 degrees of wind direction interval all data acquired during the 2-years of the study. They have to be interpreted in conjunction with the various source areas that surround Finokalia station, notably mainland Greece, central Europe (N, NW), east Europe, Turkey (NE, E), Italy and the western Mediterranean region (W), and Africa (SW, S, SE). Note also that during winter air originates mainly from the Atlantic region and during summer from polluted Europe and Turkey (Lelieveld et al., 2002). The wind speed and Radon (Figs. 3a, b) highest values were associated with the northwest sector, indicative of air mass transport from polluted continental areas. High levels of ozone (Fig. 3c) were observed for wind directions from the north-west (Greece and central Europe) and north to north-east (east Europe, Turkey). NO_2 (Fig. 3d) was also slightly enhanced when the air masses originate from the northwest sector, compared to southerlies. As shown in Fig. 2e, NO_3 radicals were 50% higher when the air masses are of north-westerly origin in comparison to all other source regions.

This dependency of the NO_3 mixing ratios on the wind direction has been further analysed for all NO_3 levels exceeding 30 pptv (in total 32 cases) during the period June 2001–September 2003 (Fig. 1). Back trajectories of the air masses reaching the sampling location, calculated by the HYSPLIT program (http://www.arl.noaa.gov/ready/hysplit4.html), are used to characterise the origin of these peaks. A high percentage (90%) of these elevated NO_3 cases is related to

air masses from the northwest-northeast sectors, while the remaining 10% has a local-mixed origin. For these 32 cases, the observed NO_3 radical mixing ratios per wind sector average 64±37 pptv (northwest), 50±38 pptv (north), 55±24 pptv (northeast) and 48±13 pptv (local and mixed).

To examine the importance of the individual chemical and meteorological factors for NO_3 radicals in detail, two characteristic cases of high NO_3 levels have been selected. Each of the 32 high NO_3 episodes observed during this study can be classified within one of these two categories (12 in case one and 20 in case two shown below).

3.1.1 Case 1: intrusion into the boundary layer

During the night of 4–5 June 2002 a rapid increase in NO_3 levels has been observed from 3 pptv to 102 pptv within 2.5 h (Fig. 4). Shortly before the NO_3 increase, the relative humidity dropped from 75 to 55%, Radon declined by about 0.8 Bq m^{-3} while ozone and NO_2 increased by about 7 ppbv and 0.2 ppbv, respectively. These observations support an intrusion event during which dry air from the free troposphere subsided into the nocturnal marine boundary layer, as identified by the trajectory analysis (Fig. 4). The air masses originated from polluted continental areas in Central Europe. The enhanced NO_3 radical mixing ratios in the free tropospheric subsiding air masses, may result from the high levels of NO_3 precursors in conjunction with depressed NO_3 losses, in particular via the N_2O_5 reaction with water vapour.

3.1.2 Case 2: transport from pollution sources

During the night of 11–12 May 2003 NO_3 radicals mixing ratio increased from 4 pptvs to 104 pptv within less than 1.5 h (Fig. 5). This rise was associated with the progressive increase in wind speed and changes in the wind direction. The back trajectory analysis reveals that these air masses had crossed the south-west coast of Turkey before reaching the sampling station. Note that under these conditions the station is receiving air masses rich in NO_2 and Radon. The relative humidity in this case did not change but remained at rather low levels (20–30%); in parallel the temperature was almost constant decreasing by only 1°C throughout the night.

The clear anti-correlation observed between O_3 and NO_2 indicates titration of O_3 by NO leading to NO_3 production. Therefore, in contrast to the earlier case when air was transported in the free troposphere and then penetrated into the boundary layer at Finokalia, in this case the air mass originated from the polluted boundary layer and was transported at lower altitudes.

3.2 Correlations between NO_3 radicals and related species-statistical analysis

Single and multiple regression analyses have been deployed to investigate the specific role of each of the factors that control the levels of NO_3 radicals such as NO_2, O_3, Radon-222,

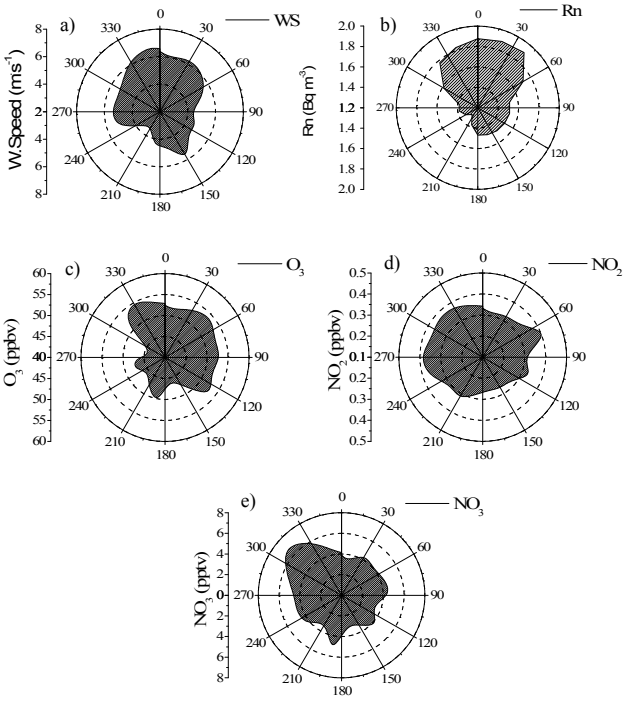

Fig. 3. Rose diagrams of the **(a)** Wind speed, **(b)** radon-222, **(c)** O_3, **(d)** NO_2 and **(e)** NO_3 as a function of wind direction at Finokalia, based on all nighttime observations integrated per 10 degree intervals of wind direction.

temperature (T), relative humidity (RH), wind direction and wind speed. The analysis is confined only to nighttime hours during which NO_3 radical mixing ratios exceed the detection limit. Specifically, more than 11 000 data points were used for the following analyses. A moving average has been additionally applied to the data series in order to subtract the seasonality (where existed) thus removing possible covariance between variables, which is due to their seasonal dependence.

3.2.1 Single regression analysis

Linear regression analysis revealed significant correlations at the 99% confidence level between NO_3 radicals and O_3 (R=0.12, N=9844), temperature (R=0.23, N=9736), relative humidity (R=−0.19, negative correlation, N=9736) and wind speed (R=0.04, N=9736). No significant correlation was found between NO_3 and NO_2. The scatter plots of NO_3 mixing ratios as function of O_3, temperature and relative humidity are shown in Figs. 6a–c. The averaged data (blue circles) for O_3, temperature and RH with the corresponding NO_3 averages do help the easier visualization of the existing relationships and fit well with the regression lines drawn (red lines) from the whole data set, obscured at first glance by the increased scattering of the values. A significant part of both O_3 and temperature correlation with NO_3 radicals is due to

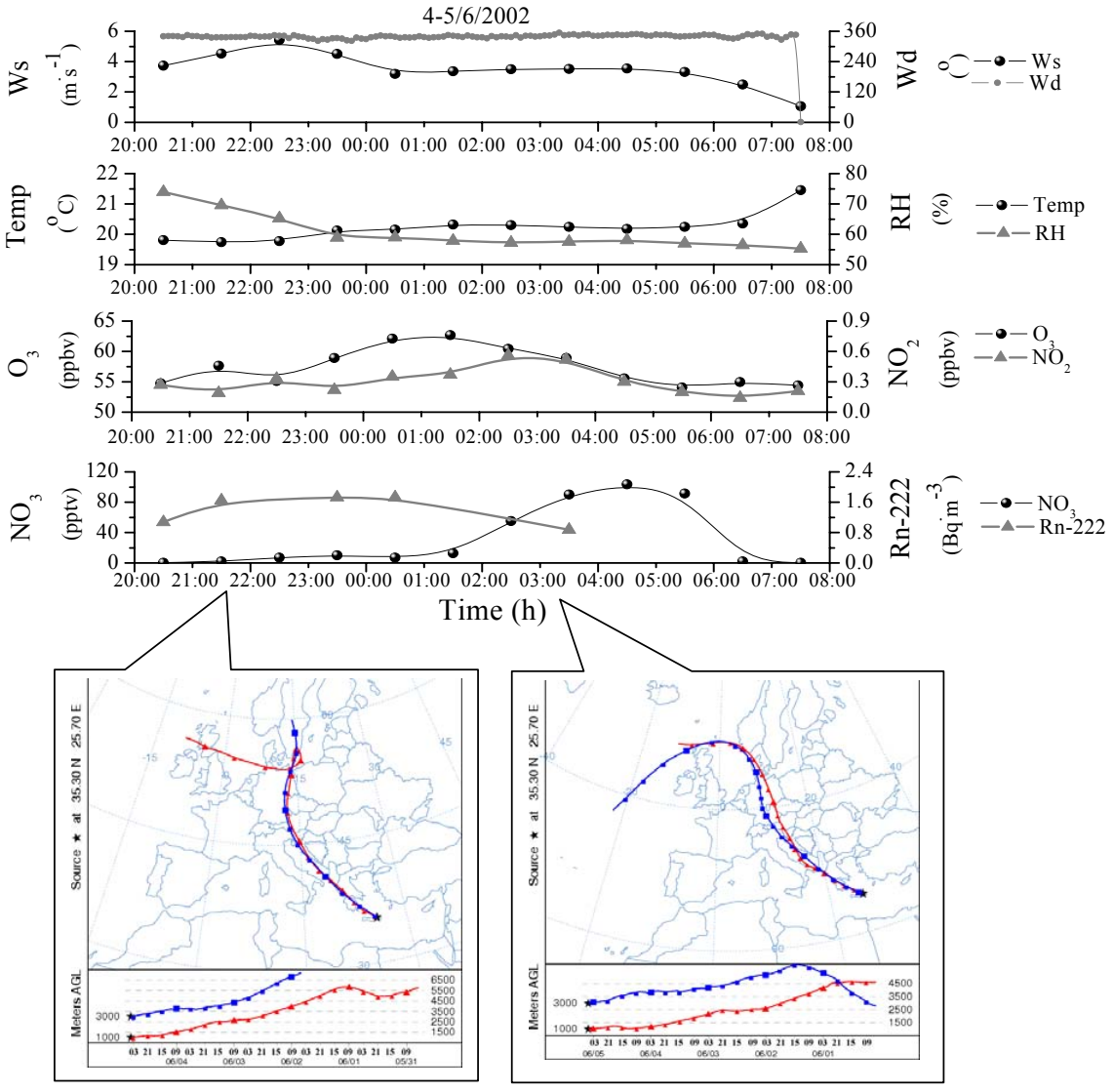

Fig. 4. Variation of wind speed, temperature, O_3 and NO_3 radicals during an intrusion of free tropospheric air masses associated with a decrease in Radon and relative humidity and increases of O_3 and NO_3 radicals (time expressed in local time), and 5-day back trajectories of air masses arriving at Finokalia on 4 June 2002 at 21:00 LT and on 5 June 2002 at 03:00 LT.

their common seasonality. This is supported by the fact that when the residuals of the ozone and temperature are used for the correlations with NO_3 (residuals derived by subtraction of the annual cycle of the series simulated by fitting the sum of a sine and its first harmonic to the data), the correlation coefficients are lower and equal 0.08 and 0.17, respectively.

3.2.2 Multiple regression analysis

To evaluate the relative importance of each parameter for the NO_3 mixing ratios a multiple regression analysis has been performed. Based on the single regression analysis results, O_3, T, RH and wind speed have been chosen as individual variable-parameters. Among them, wind speed has been rejected by the model at the 95% confidence level (alpha=0.05). The analysis has been repeated with O_3, RH and T, after eliminating the outliers. These outliers have been identified via residual analysis between the predicted and initial NO_3 values with the criterion of the ± 2 sigma. The derived linear correlation that expresses the NO_3 variability is:

$$NO_3 = (1.2 \pm 0.4)10^{-5} \cdot O_3 + (0.18 \pm 0.01) \cdot T + (-0.030 \pm 0.003) \cdot RH + (-48 \pm 3) \quad (1)$$

where NO_3 in pptv, O_3 in pptv, T in K and RH in %, regression coefficients are accompanied by their respective standard errors.

The R^2 (0.072, N=8943) indicates that 7.2% of the variability of NO_3 radicals can be explained by the above 3

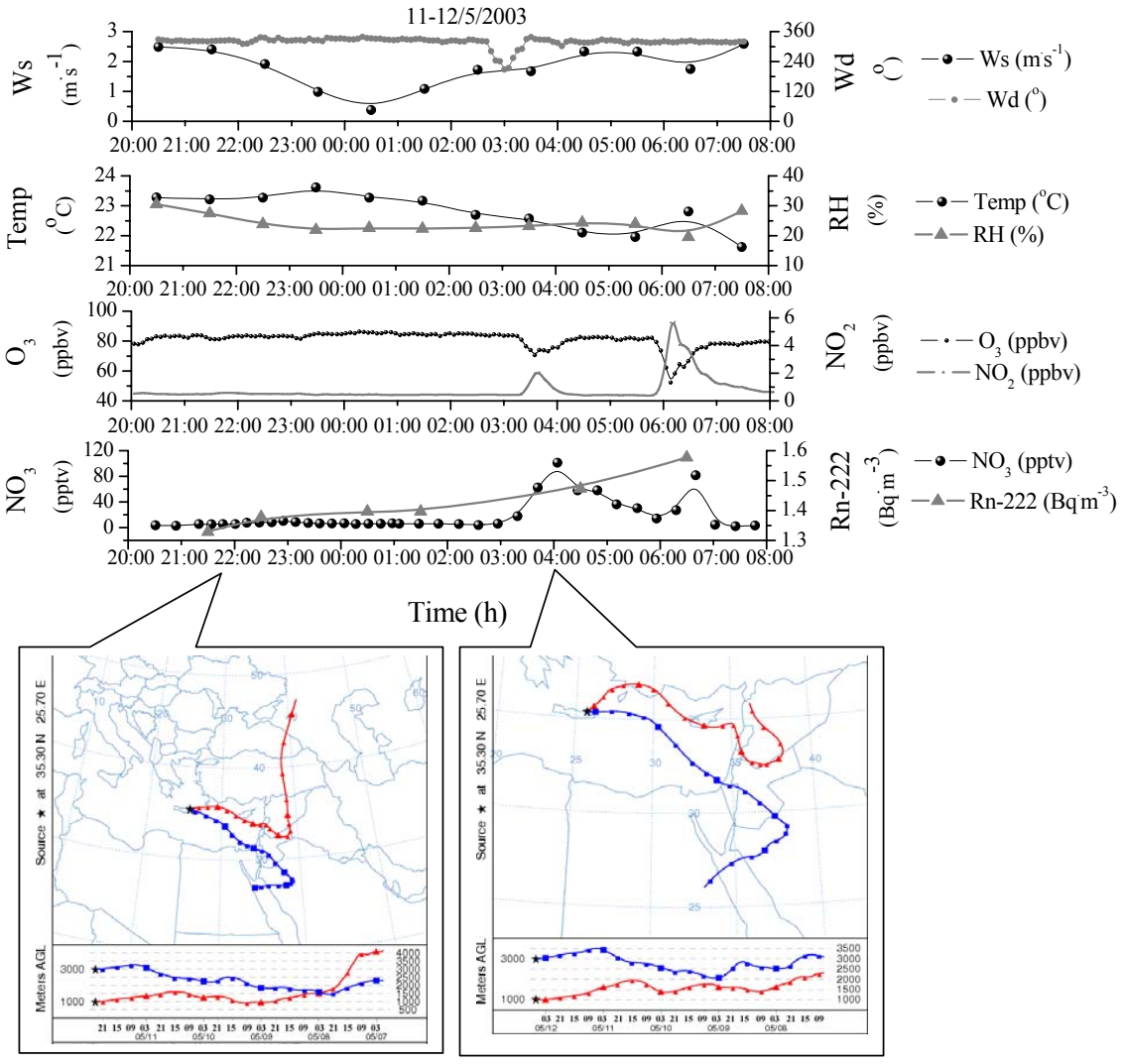

Fig. 5. Variation of wind speed, temperature, O_3 and NO_3 radicals during Transport of polluted air masses as indicated by an increase in Radon, and wind speed, change in wind direction followed by and increase in NO_2 and depletion of O_3, an increase in NO_3 radicals (time expressed in local time) and 5-day back trajectories of air masses arriving at Finokalia on 11 May 2003 at 22:00 LT and on 12 May 2003 at 04:00 LT.

variables. This explained variability is related by 60%, 30% and 10% to the T, the RH and the O_3 variability, respectively.

The results of both single and multiple regression analyses show that the NO_3 radicals are very sensitive to changes in temperature and relative humidity and, to a lesser extent, to O_3 variations. Relative humidity is the only parameter anti-correlated with NO_3 due to the indirect removal via heterogeneous reactions of N_2O_5, as will be discussed below.

3.3 Factors controlling NO_3 levels – mechanistic studies

Under steady state conditions the NO_3 levels are in equilibrium between production (P_{NO3}) and losses (f_{NO3}). The production rate of NO_3 radicals by Reaction (R1) is given by

$$P_{NO_3} = k_{NO_2+O_3} \cdot [NO_2][O_3] \quad (2)$$

where $k_{NO_2+O_3}$ is the rate of this reaction. The losses of NO_3 radicals (f_{NO3}) are the sum of direct (f_A) and indirect loss rates (f_B).

$$f_{NO_3} = f_A + f_B = \frac{P_{NO_3}}{[NO_3]} \quad (3)$$

The indirect losses of NO_3 (f_B) are related to the loss of N_2O_5 (f_B') as shown below in Eq. (4) that is derived assuming steady-state conditions for N_2O_5, NO_3 (Geyer et al., 2001b):

$$[NO_3] = \frac{P_{NO_3}}{f_A + [NO_2] \cdot k_{eq} \cdot f'_B} \quad (4)$$

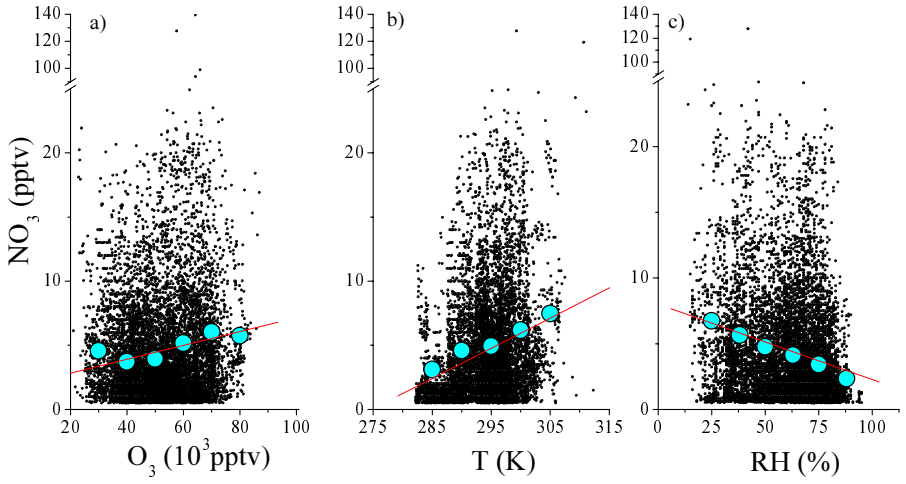

Fig. 6. Scatter plots of NO_3 mixing ratios (in pptv) as a function of **(a)** Ozone (in 10^3 pptv), **(b)** Temperature (in K) and **(c)** Relative Humidity (in %). Blue circles are data averaged every 10^4 pptv (for O_3), 5 K (for temperature) and 12.5% (for RH).

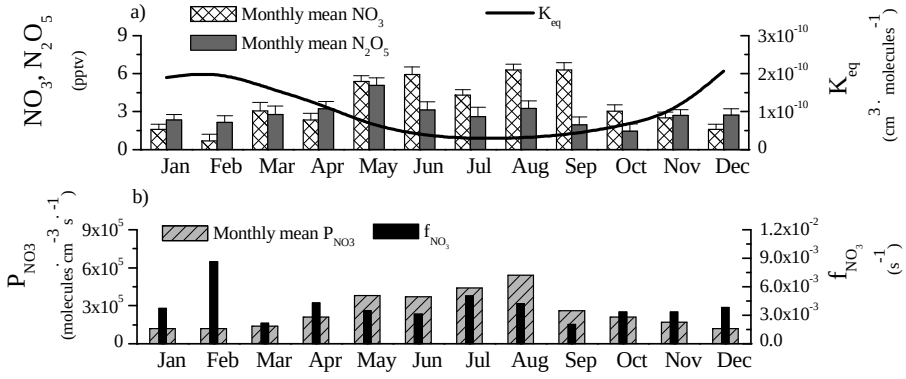

Fig. 7. Annual cycle **(a)** of observed NO_3 and of N_2O_5 (left axis) calculated assuming steady-state conditions and no heterogeneous losses and of the equilibrium constant K_{eq} of the Reactions [3,-3] (right axis) given by $k_{eq}=3\times10^{-27}$ exp(10 990/T) (Sander et al., 2003) **(b)** of the production (P_{NO3}: left axis) and the loss rate (f_{NO3}: see text; right axis) of NO_3 radicals; monthly mean values and standard deviations based on the June 2001 to September 2003 observations.

where

$$k_{eq}=\frac{k_{NO2+NO3}}{k_{-(N2O5)}}=\frac{[N_2O_5]}{[NO_2]\cdot[NO_3]} \quad (5)$$

The N_2O_5 levels can be calculated based on the observed NO_3 and NO_2 levels, and the temperature dependent equilibrium constant k_{eq} of the reversible reaction (Reaction R(3,−3)). For the whole sampling period monthly averages for N_2O_5, P_{NO3}, and f_{NO3} are shown in Fig. 7. In winter when temperatures are low, k*eq* (Fig. 7a) is high thus shifting the equilibrium towards N_2O_5 and increasing the importance of N_2O_5 losses over the direct losses of NO_3. In addition, our wintertime observations indicate a very efficient loss of NO_3 (f_{NO3}: sum of direct and indirect losses; Fig. 7b) that drastically suppresses the bulk NO_3 and N_2O_5 pool levels and as will be discussed in Sect. 3.3.2 is related to the indirect sink of NO_3 radicals. Therefore, N_2O_5 monthly mean levels calculated assuming steady-state conditions (Fig. 7a) present maxima in late spring and early summer.

From Eqs. (3) and (4) we deduce that the slope of $[NO_3]$ against P_{NO3} equals the turnover time of NO_3 considering both the direct and the indirect losses of NO_3.

$$\tau_{NO_3}=\frac{1}{f_A+[NO_2]\cdot k_{eq}\cdot f'_B} \quad (6)$$

If the indirect losses are negligible ($f_B\approx0$), $[NO_3]$ should be directly proportional to the P_{NO3} (significant correlation) and, then, the slope of the linear relationship between $[NO_3]$ and P_{NO3} that equals the lifetime of NO_3 radicals (τ_{NO3}) is f_A^{-1}. On the other hand, if the direct losses are negligible ($f_A\approx0$) and the indirect NO_3 loss predominates, the above equation leads to

$$\tau_{NO_3}=\frac{1}{[NO_2]\cdot k_{eq}\cdot f'_B} \quad (7)$$

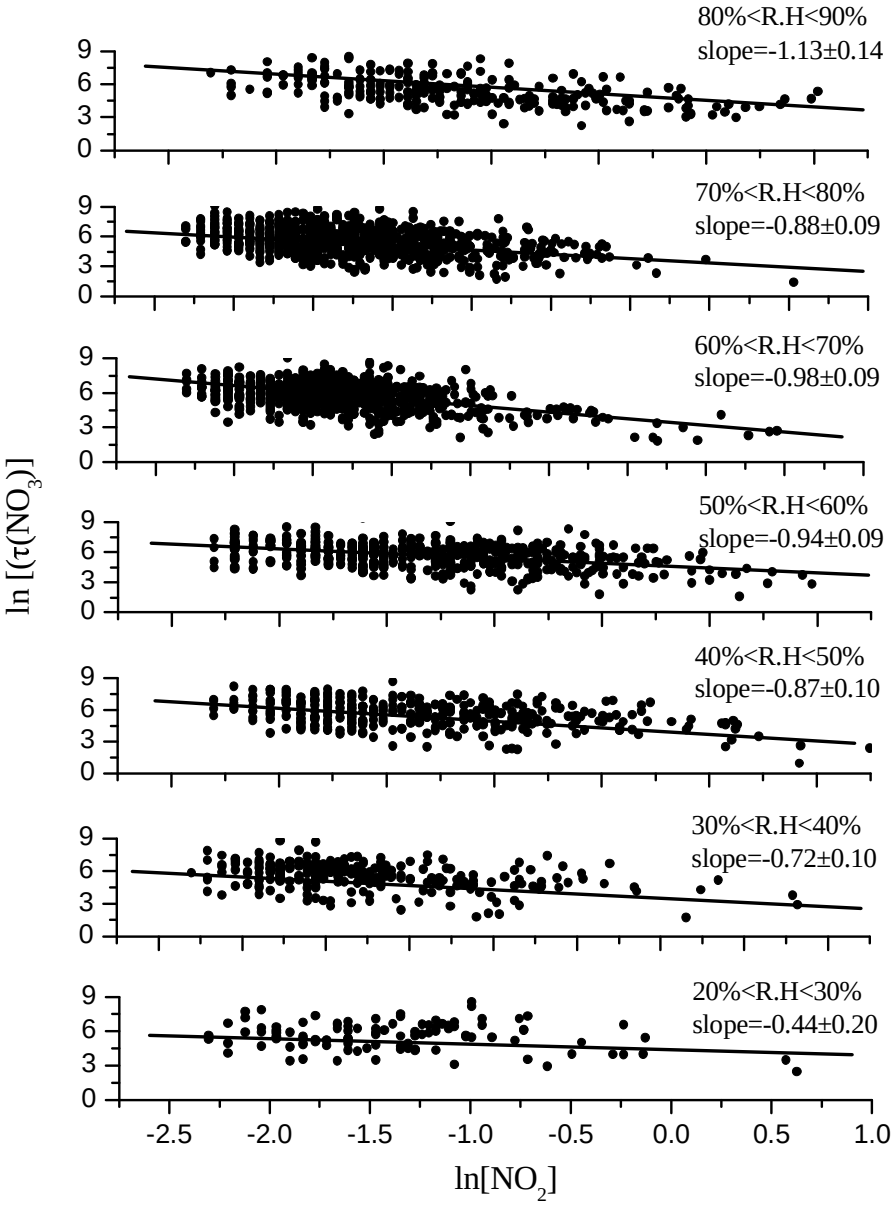

Fig. 8. Correlation of the logarithm of the lifetime of NO_3 radicals as deduced from observations and the logarithm of NO_2 mixing ratios at 7 different relative humilities ranges (from 20% to 90% every 10%). Slopes closer to -1 indicate higher involvement of the indirect losses of NO_3.

Then τ_{NO3} is proportional to the inverse of the NO_2 mixing ratio (or $\ln(\tau_{NO3})=-\ln(k_{eq}\ f'_B\ [NO_2])$).

Below the production and loss rates of NO_3 will be examined in detail.

3.3.1 Production rate of the NO_3

Based on Eq. (2) and the temperature dependence of the reaction rate $k_{NO_2+O_3}=1.4\times10^{-13}\cdot\exp\left[-\frac{2490}{T}\right]$ cm^3 molecules^{-1} s^{-1} (T in K; Atkinson et al., 2004), under typical conditions in the Mediterranean area during summer ([NO_2]=0.5 ppbv, and [O_3]=50 ppbv, T=298 K) the production rate of NO_3 (P_{NO_3}) equals 4.9×10^5 molecules cm^{-3} s^{-1} (or 72 pptv NO_3 per hour). Assuming dynamic equilibrium of NO_3 (i.e. that the production by Reaction (R1) equals the loss by photo-dissociation (Reactions (R2a) and (R2b)) and reaction with NO, for average summer daytime [NO]=0.05 ppbv and $k_{NO_3+NO}=1.8\times10^{-11}\cdot\exp\left[\frac{110}{T}\right]=2.6\times10^{-11}$ cm^3

Table 2. Indicators of direct (a) and indirect (b) NO_3 losses and corresponding lifetimes (τ_A and τ_B, respectively). (a) Linear correlation of the NO_3 radicals mixing ratio with the NO_3 production rate (P_{NO3}), and (b) linear correlation of the logarithm of the NO_3 lifetime (τ_{NO3}) with the logarithm of the NO_2 mixing ratio. The linear slope of the direct sinks represents the NO_3 lifetime, τ_A, τ_B are calculated from the seasonal (or annual) NO_2 values and the corresponding logarithmic equation presented in the table.

NO_3 values are expressed in molecules cm^{-3}, P_{NO3} in molecules cm^{-3} s^{-1}, NO_2 in ppbv, τ_{NO3} in s.

Period	$[NO_3]=f(P_{NO3})$ Slope (r^2)	τ_A (min)	$\ln[\tau_{NO3}]=f(\ln[NO_2])$ $y=ax+b$ (r^2)	τ_B (min)
Year	300*±41(0.41)	5.0	y=(−1.0±0.4)x+(4.6±0.1) (0.93)	5.4
Winter	174±20 (0.08)	2.9	y=(−1.5±0.7)x+(2.8±0.6) (0.78)	2.3
Spring	520±26(0.96)	8.6	y=(−0.8±0.4)x+(5.1±0.3) (0.38)	7.5
Summer	203±33 (0.10)	3.4	y=(−1.1±0.1)x+(4.9±0.1) (0.88)	6.1
Summer_1	321±41 (0.99)	5.4	y=(−0.6±0.1)x+(5.5±0.1) (0.95)	7.1
Summer_2	106±29 (0.10)	1.8	y=(−1.2±0.3)x+(4.9±0.1) (0.78)	6.7
Autumn	200±50 (0.25)	3.3	y=(−1.4±0.4)x+(3.3±0.2) (0.92)	2.3
Autumn_1	649±152(0.75)	10.8	y=(−0.8±0.1)x+(4.6±0.1) (0.97)	4.2
Autumn_2	128±40 (0.35)	2.1	y=(−1.6±0.5)x+(3.7±0.2) (0.94)	4.4

*experimentally deduced see text.

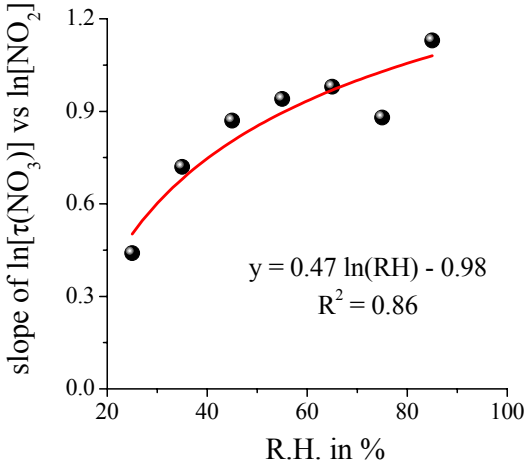

Fig. 9. Correlation of the slope of the regression of ln[τ(NO3)] versus the ln[NO_2] (data from Fig. 8) as a function of RH.

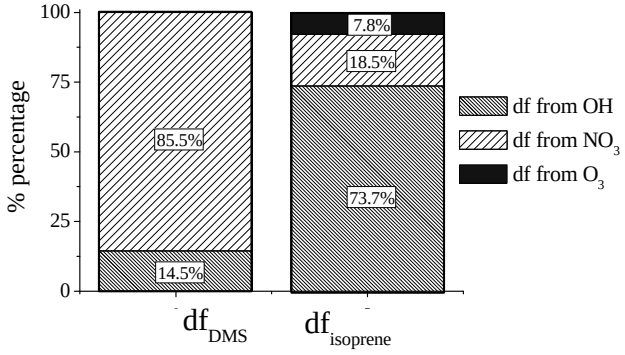

Fig. 10. Contribution of the 3 major oxidants, OH, NO_3 and O_3 to the annual mean degradation frequencies of DMS and isoprene for the studied area.

molecules^{-1} s^{-1}, the steady-state daytime concentration of NO_3 is calculated to be about 0.1 pptv. Maximum temperature differences of 40°C that have been observed between summer and winter can change P_{NO3} by a factor of 3.5 (higher P_{NO3} during summer) assuming that the levels of NO_2 and O_3 do not change significantly. However, the monthly mean temperatures differ by about 14°C between summer and winter (Vrekoussis et al., 2006). In addition, NO_2 and O_3 mixing ratios are higher during summer than during winter. Thus, the overall effect is that the nitrate radical production (P_{NO3}) is about 4 times faster during summer than during winter. The annual mean P_{NO3} derived from the monthly averages equals $(2.6\pm1.4)\times10^5$ molecules cm^{-3} s^{-1} (Fig. 7). Note that P_{NO3} calculated over the 5 min sampling time shows two orders of magnitude variability, ranging from 5.0×10^4 molecules cm^{-3} s^{-1} to 5.5×10^6 molecules cm^{-3} s^{-1}.

3.3.2 Losses of NO_3

Direct removal of NO_3 concerns the NO_3 reactions mainly with VOC, including DMS naturally emitted by the ocean, and with peroxy (RO_2) radicals. The indirect removal of NO_3 occurs via N_2O_5 formation and subsequent heterogeneous reactions.

For the following analysis, to reduce the high scatter in the NO_3 data set (more than 15 000 measurements), NO_3 have been averaged per unit of P_{NO3} equal to 1×10^5 molecules cm^{-3} s^{-1} and τ_{NO3} (equal to $1/f_{NO3}$) has been averaged per unit of NO_2 equal to 100 pptv. The interpretation of all data, according to the above analysis for the direct sinks, leads to a linear regression

$$[NO_3]=300\cdot P_{NO3}\ (r^2=0.41) \quad (8)$$

whereas the derived equation for the indirect sinks is:

$$\ln(\tau_{NO3}) = -1.02 \ln[NO_2] + 4.6 (r^2=0.93) \quad (9)$$

where NO_3 values are expressed in molecules cm^{-3}, P_{NO3} in molecules $cm^{-3}\,s^{-1}$, NO_2 in ppbv, τ_{NO3} in s.

These results indicate relatively strong indirect losses in this region during the 2-years period.

However there is also significant seasonal variability in the importance of the direct versus the indirect NO_3 loss pathways as indicated by the seasonally resolved correlations (Table 2). During winter the direct sinks of NO_3 radicals are of little importance contrary to the indirect ones whereas during spring the data reveal a strong linear correlation (r^2=0.96) between NO_3 radicals and their production rate indicating dominance of the direct losses of NO_3. Significant correlations between NO_3 radicals and their production rate have been also determined for summer and to a lesser extend for autumn.

Indeed, a closer examination of the dataset for these seasons reveals two sub-sets. The one sub-set corresponds to a higher linear regression slope and a significant correlation between P_{NO3} and NO_3, whereas the second one does not present any significant correlation between P_{NO3} and NO_3 (Table 2). The first one, with a high production rate P_{NO3} and high NO_3 mixing ratios, corresponds to steady-state conditions in the area where the direct sinks of NO_3 are important, most probably due to increased VOC concentrations from biogenic emissions, indicating dominance of direct NO_3 losses. The second subset is linked to high P_{NO3}, high NO_2 and low NO_3 mixing ratios. In addition, for this subset the slope of $\ln(\tau_{NO3})$ versus $\ln[NO_2]$ is significantly more negative than the respective of the subset one, thus, suggesting indirect sinks for the NO_3 radicals. These slopes have to be viewed with caution since due to the large variability of the observations the slopes are associated with high uncertainties that can generate absolute values higher than unity.

The above analysis is coherent with observations of biogenic organic compounds in the area that are reactive against NO_3 radical. These observations indicate enhanced levels of isoprene during spring and summer (Liakakou et al., 2007) and of marine dimethylsulfide (DMS) from spring to autumn (Kouvarakis and Mihalopoulos, 2002). However, lack of simultaneous measurements of NO_3 radicals and biogenic organic compounds prohibits any deeper analysis of our data.

To further investigate the importance of the heterogeneous chemistry in NO_3 removal via the reactions of N_2O_5, the methodology applied by Heintz et al. (1996) has been followed. The logarithmic correlation between the NO_3 lifetime and the NO_2 concentration is considered for 7 different ranges of relative humidity from 20 to 90% every 10% (Fig. 8). It is found that the slope approaches the "ideal" value of -1 at high relative humidity. Indeed the slope of ln[t(NO3)] vs ln[NO2] exhibits a nice logarithmic relationship with RH (Fig. 9; R^2=0.856, N=7) that further supports the existence of indirect sinks for NO_3 that are strongly related to the presence of water vapour in the atmosphere. This clearly indicates the increasing importance of N_2O_5 hydrolysis with increasing RH and thus water vapour in the atmosphere.

3.4 Implications of the observations

Based on our observations, during nighttime the annual median steady-state NO_3 lifetime is estimated to be about 5 min and presents large temporal variability (up to a factor of 5) shown in Table 2.

Taking into account the observed levels of NO_3 radicals, several VOC species are subject to important nighttime chemistry initiated by NO_3, i.e. of similar relevance as daytime chemistry driven by OH radicals (Vrekoussis et al., 2004). Indeed, for the studied area, based on the observed NO_3 levels and the OH radicals observed during summer 2001 (Berresheim et al., 2003) and calculated for the other seasons (Vrekoussis et al., 2006), the NO_3 initiated nighttime VOC oxidation appears to be more important than the daytime oxidation by OH radicals for a number of VOCs, particularly for monoterpenes and DMS. For these two volatile organic compounds of biogenic origin, isoprene and dimethylsulfide that have been measured in the area (Liakakou et al., 2007; Kouvarakis and Mihalopoulos, 2002), the degradation frequencies have been calculated based on the observed seasonally averaged NO_3, O_3 and temperature levels and the modelled OH for the area (Vrekoussis et al., 2006). The derived annual mean degradation frequencies for the area (Fig. 10) indicate that NO_3 radicals are almost 6 times more efficient than OH radicals in destroying DMS. For isoprene degradation, OH radicals are almost 4 times more efficient than NO_3 and 10 times more efficient than O_3 that contributes by about 8% to the degradation frequency of isoprene on an annual basis. In turn, our model calculations (Vrekoussis et al., 2006; Liakakou et al., 2007) indicate that in the area in the marine boundary layer DMS and isoprene contribute by about 5% and 20%, respectively, to the annual mean NO_3 degradation frequency during night. Thus, VOC oxidation can lower NO_3 levels and shorten NO_3 lifetime. These results agree with recent observations of a positive NO_3 radical vertical gradient in the mid-latitude coastal marine boundary layer during summer (Saiz-Lopez et al., 2006). These authors have explained their observations by a potentially efficient removal of NO_3 radicals by DMS.

In addition, the NO_3 initiated oxidation of VOCs contributes to the nighttime formation of OH and peroxy radicals (Platt et al., 1990; Vrekoussis et al., 2007[1]). Finally, our results underscore that nighttime chemistry initiated by NO_3

[1]Vrekoussis, M., Myriokefalitakis, S., Mihalopoulos, N., Kanakidou, M., et al.: Nighttime occurrence of peroxy radicals in the anthropogenically influenced marine boundary layer, in preparation, 2007.

radicals is as important as daytime chemistry for the formation of nutrient, nitrate as discussed in detail by Vrekoussis et al. (2006).

4 Conclusions

This paper presents the first long-term NO_3 radical observations performed by a DOAS instrument in the marine boundary layer in the eastern Mediterranean region for a two-year period. The observed nighttime NO_3 levels vary between the detection limit of the instrument (about 1.2 pptv) and 139 pptv with seasonal averages that have a maximum in summer (5.6±1.2 pptv) and a minimum in winter (1.2±1.2 pptv); and an annual mean value of 4.2±2.3 pptv.

Single and multiple component regression analyses on the large number of simultaneous observations demonstrate temperature (positive correlation) and relative humidity (negative correlation) as the most important factors controlling NO_3 levels, and to a lesser extend O_3. However, a significant part of NO_3 and temperature covariance is linked to their seasonal variation.

Further data analysis points to the indirect loss of NO_3 via conversion to N_2O_5, followed by heterogeneous reactions as the major loss process for NO_3 year-around. Direct losses of NO_3 are shown to be important in spring and some summer and autumn periods with high biogenic emissions. Our results also indicate that NO_3 radicals can be important for nighttime VOC oxidation, contributing to the nighttime formation of peroxy radicals, nitric acid and particulate nitrate and in turn biogenic VOC significantly contribute to the NO_3 degradation frequency during night.

Acknowledgements. The authors acknowledge valuable help with the DOAS instrument logistics by D. Perner and T. Kluepfel. M. Vrekoussis has been supported by a PENED grant. Presentation of the work has been facilitated by the ACCENT EU Network of Excellence. At its latest stage this project has been supported by European Social Funds and National Resources EPEAEK II-PYTHAGORAS. This paper is dedicated to the memory of G. Hönninger from the University of Heidelberg, who performed the first DOAS measurements at Finokalia station during the ELCID campaign (June 2000).

Edited by: F. J. Dentener

References

Allan, B. J., Carslaw, N., Coe, H., Burgess, R., and Plane, J. M. C.: Observations of the Nitrate Radical in the marine boundary layer, J. Atmos. Chem., 33, 129–154, 1999.

Allan, B. J., Mc Figgans, G., Plane, J. M. C., Coe, H., and Mc Fadyen, G. G.: The nitrate radical in the remote marine boundary layer, J. Geophys. Res., 105(D19), 24 191–24 204, 2000.

Atkinson, R.: Atmospheric chemistry of VOCs and NOx, Atmos. Environ., 34(12–14), 2063–2101, 2000.

Atkinson, R., Baulch, D. L., Cox, R. A., Crowley, J. N, Hampson, R. F., Kerr, J. A., Rossi, M. J., and Troe, J.: IUPAC recommendations, Web version, http://www.iupac-kinetic.ch.cam.ac.uk, 2003.

Atkinson, R., Baulch, D. L., Cox, R. A., Crowley, J. N., Hampson, R. F., Hynes, R. G., Jenkin, M. E., Rossi, M. J., and Troe, J.: Evaluated kinetic and photochemical data for atmospheric chemistry: Volume I – gas phase reactions of O_x, HO_x, NO_x and SO_x species, Atmos. Chem. Phys., 4, 1461–1738, 2004, http://www.atmos-chem-phys.net/4/1461/2004/.

Badger, C. L., Griffiths, P. T., George, I., Abbatt, J. P. D., and Cox, R. A.: Reactive uptake of N_2O_5 by aerosol particles containing mixtures of humic acid and ammonium sulphate, J. Phys. Chem. A, 110(21), 6986–6994, 2006.

Berresheim, H., Plass-Dülmer, C., Elste, T., Mihalopoulos, N., and Rohrer, F.: OH in the coastal boundary layer of Crete during MINOS: Measurements and relationship with ozone photolysis, Atmos. Chem. Phys., 3, 639–649, 2003, http://www.atmos-chem-phys.net/3/639/2003/.

Brown, S. S., Stark, H., Ryerson, T. B., Williams, E. J., Nicks Jr., D. K., Trainer, M. , Fehsenfeld, F. C., and Ravishankara, A. R.: Nitrogen oxides in the nocturnal boundary layer: Simultaneous in situ measurements of NO_3, N_2O_5, NO_2, NO, and O_3, J. Geophys. Res., 108(D9), 4299, doi:10.1029/2002JD002917, 2003.

Brown, S. S., Dibb, J. E., Stark, H., Aldener, M., Vozella, M., Whitlow, S., Williams, E. J., Lerner, B. M., Jakoubek, R., Middlebrook, A. M, DeGouw, J. A., Warneke, C., Goldan, P. D., Kuster, W. C., Angevine, W. M., Sueper, D. T., Quinn, P. K., Bates, T. S., Meagher, J. F., Fehsenfeld, F. C., and Ravishankara, A. R.: Nighttime removal of NO_x in the summer marine boundary layer, Geophys. Res. Lett., 31, L07108, doi:10.1029/2004GL019412, 2004.

Brown, S. S., Ryerson, T. B., Wollny, A. G., Brock, C. A., Peltier, R., Sullivan, A. P., Weber, R. J., Dube, W. P., Trainer, M., Meagher, J. F., Fehsenfeld, F. C., and Ravishankara, A. R.: Variability in nocturnal nitrogen oxide processing and its role in regional air quality, Science, 311(5757), 67–70, 2006.

Carslaw, N., Plane, J. M. C., Coe, H., and Cuevas, E.: Observation of the nitrate radical in the free troposphere. J. Geophys. Res., 102(D9), 10 613–10 622, 1997a.

Carslaw, N., Carpenter, L. J., Plane, J. M. C., Allan, B. J., Burgress, R. A., Clemitshaw, K. C., Coe, H., and Penkett, S. A.: Simultaneous observations of nitrate and peroxy radicals in the marine boundary layer, J. Geophys. Res., 102(D15), 18 917–18 934, 1997b.

Gerasopoulos, E., Kouvarakis, G., Vrekoussis, M., Kanakidou, M., and Mihalopoulos, N.: Ozone variability in the marine boundary layer of the Eastern Mediterranean based on 7-year observations, J. Geophys. Res., 110, D15309, doi:10.1029/2005JD005991, 2005.

Gerasopoulos, E., Kouvarakis, G., Vrekoussis, M., Donoussis, Ch., Mihalopoulos, N., and Kanakidou, M.: Photochemical ozone production in the Eastern Mediterranean, Atmos. Environ., 40, 3057–3069, 2006.

Geyer, A., Ackermann, R., Dubois, R., Lohrmann, B., Muller, T., and Platt, U.: Long term observation of Nitrate radicals in the continental layer near Berlin., Atmos. Environ., 35, 3619–3631, 2001a.

Geyer, A., Alicke, B., Konrad, S., Schmitz, T., Stutz, J., and Platt,

U.: Chemistry and oxidation capacity of the nitrate radical in the continental boundary layer near Berlin, J. Geophys. Res., 106(D8), 8013–8025, 2001b.

Heintz, F., Platt, U., Flentje, H., and Dubois, R.: Long term observation of Nitrate radicals at the Tor Stations, Kap Arkona (Rügen), J. Geophys. Res., 101(D17), 22 891–22 910, 1996.

Hu, J. H. and Abbatt, J. P. D.: Reaction Probabilities for N_2O_5 hydrolysis on sulfuric acid and ammonium sulphate aerosols at room temperatures, J. Phys. Chem., 101(5), 871–878, 1997.

Kourtidis, K., Zerefos, C., Rapsomanikis, S., Simeonov, V., Balis, D., Perros, P. E., Thompson, A. M., Witte, J., Calpini, B., Sharobiem, W. M., Papayannis, A., Mihalopoulos, N., and Drakou, R.: Regional levels of ozone in the troposphere over eastern Mediterranean, J. Geophys. Res., 107(D18), doi:10.1029/2000JD000140, 8140, 2002.

Kouvarakis, G., Tsigaridis, K., Kanakidou, M., and Mihalopoulos, N.: Temporal variations of surface regional background ozone over Crete Island in the southeast Mediterranean, J. Geophys. Res., 105(D4), 4399–4407, 2000.

Kouvarakis, G., Vrekoussis, M., Mihalopoulos, N., Kourtidis, K., Rappenglueck, B., Gerasopoulos, E., and Zerefos, C.: Spatial and temporal variability of tropospheric ozone (O-3) in the boundary layer above the Aegean Sea (eastern Mediterranean), J. Geophys. Res.-Atmos., 107(D18), 8137, doi:10.1029/2000JD000081, 2002.

Kouvarakis, G. and Mihalopoulos, N.: Seasonal variation of dimethylsulfide in the gas phase and of methanesulfonate and non-sea-salt sulfate in the aerosols phase in the Eastern Mediterranean atmosphere, Atmos. Environ., 36, 929–938, 2002.

Lelieveld, J., Berresheim, H., Borrmann, S., Crutzen, P. J., Dentener, F. J., Fischer, H., Feichter, J., Flatau, P. J., Heland, J., Holzinger, R., Korrmann, R., Lawrence, M. G., Levin, Z., Markowicz, K. M., Mihalopoulos, N., Minikin, A., Ramanathan, V., de Reus, M., Roelofs, G.-J., Scheeren, H. A., Sciare, J., Schlager, H., Schultz, M., Siegmund, P., Steil, B., Stephanou, E. G., Stier, P., Traub, M., Warneke, C., Williams, J., and Ziereis, H.: Global air pollution crossroads over the Mediterranean, Science, 298(5594), 794–799, 2002.

Liakakou, E., Vrekoussis, M., Bonsang, B., Donousis, Ch., Kanakidou, M., and Mihalopoulos, N.: Isoprene above the Eastern Mediterranean: Seasonal variation and contribution to the oxidation capacity of the atmosphere, Atmos. Environ., 41(5), 1002–1010, doi:10.1016/j.atmosenv.2006.09.034, 2007.

Martinez, M., Perner, D., Hackenthal, E.., Kultzer, S., and Schultz, L.: NO_3 at Helgoland during the NORDEX campaign in October 1996, J. Geophys. Res., 105(D18), 22 685–22 695, 2000.

Mihalopoulos, N., Stephanou, E., Kanakidou, M., Pilitsidis, S., and Bousquet, P..: Tropospheric aerosol ionic composition in the Eastern Mediterranean region, Tellus B, 49(3), 314–326, 1997.

Orlando, J. J., Tyndall, G. S., Moortgat, G. K., and Calvert, J. G.: Quantum Yields For NO_3 Photolysis Between 570 and 635 nm, J. Phys. Chem., 97(42), 10 996–11 000, 1993.

Platt, U., Perner, D., Winer, A. M., Harris, G. W., and Pitts, J. N.: Detection of NO_3 in the polluted troposphere by differential optical absorption, Geophys. Res. Lett., 7, 89–92, 1980.

Platt, U. and Perner, D.: Measurements of atmospheric trace gases by long path differential uv/visible absorption spectroscopy, in: Optical and Laser remote Sensing, vol. 39, edited by: Killinger, D. K. and Mooradian, A., Springer Ser., Optical Sci., pp 95–105, 1983.

Platt, U., Le Bras, G., Poulet, G., Burrows, J. P., and Moortgat, G.: Peroxy-Radicals From Nighttime Reaction Of NO_3 With Organic-Compounds, Nature, 348(6297), 147–149. 1990.

Rudich, Y., Talukdar, R. K., and Ravishankara, A. R.: Reactive uptake of NO_3 on pure water and ionic solutions, J. Geophys. Res.-Atmos., 101(D15), 21 023–21 031, 1996.

Saiz-Lopez, A., Shillito, J. A., Coe, H., and Plane, J. M. C.: Measurements and modelling of I_2, IO, OIO, BrO and NO_3 in the mid-latitude marine boundary layer, Atmos. Chem. Phys., 6, 1513–1528, 2006, http://www.atmos-chem-phys.net/6/1513/2006/.

Salisbury, G., Rickard, A. R., Monks, P. S., Allan, B. J., Bauguitte, S., Penkett, S. A., Carslaw, N., Lewis, A. C., Creasey, D. J., Heard, D. E., Jacobs, P. J., and Lee, J. D.: Production of peroxy radicals at night via reactions of ozone and the nitrate radical in the marine boundary layer, J. Geophys. Res.-Atmos., 106(D12), 12 669–12 687, 2001.

Sander, S. P., Friedl, R. R., Ravishankara, A. R., Golden, D. M., Kolb, C. E., Kurylo, M. J., Huie, R. E., Orkin, V. L., Molina, M. J., Moortgat G. K., and Finlayson-Pitts, B. J.: Chemical Kinetics and Photochemical Data for Use in Atmospheric Studies, Evaluation Number 14, JPL Publication 02-25, NASA, 2003.

Schutze, M. and Herrmann, H.: Determination of phase transfer parameters for the uptake of HNO_3, N_2O_5 and O_3 on single aqueous drops, Phys. Chem. Chem. Phys., 4(1), 60–67, 2002.

Sebastián Müller-de Vries, O.: The relative contribution of free radicals to the oxidation chain of dimethylsulphide in the marine boundary layer, PhD Thesis, University of Heidelberg, Germany, 188 pp., 2005.

Thomas, K., Volz-Thomas, A., Mihelcic, D., Smit, H. G. J., and Kley, D.: On the exchange of NO_3 radicals with aqueous solutions: Solubility and sticking coefficient, J. Atmos. Chem., 29(1), 17–43, 1998.

Vrekoussis, M., Kanakidou, M., Mihalopoulos, N., Crutzen, P. J., Lelieveld, J., Perner, D., Berresheim, H., and Baboukas, E.: Role of the NO_3 radicals in the oxidation processes in the eastern Mediterranean troposphere during the MINOS campaign, Atmos, Chem, Phys., 4, 169–182, 2004.

Vrekoussis, M., Liakakou, H., Mihalopoulos, N., Kanakidou, M., Crutzen, P. J., and Lelieveld J.: Formation of HNO_3 and NO_3^- in the anthropogenically-influenced eastern Mediterranean marine boundary layer, Geophys. Res. Lett., 33, L05811, doi:10.1029/2005GL025069, 2006.

Wahner, A., Mentel, T. F., and Sohn, M.: Gas-phase reaction of N_2O_5 with water vapor: Importance of heterogeneous hydrolysis of N_2O_5 and surface desorption of HNO_3 in a large teflon chamber, Geophys. Res. Lett., 25(12), 2169–2172, 1998.

Yokelson, R. J., Burkholder, J. B., Fox, R. W., Talukdar, R. K., and Ravisankara, A. R.: Temperature dependence of the NO_3 radical, J. Phys. Chem., 98, 13 144–13 150, 1994.

Yoshino, K., Esmond., J. R., and Parkinson, W. H.: High resolution absorption cross section measurements of NO_2 in the UV and VIS region, Chem. Phys., 221, 169–174, 1997.

Zetsch, C. and Behnke, W.: Heterogeneous photochemical sources of atomic Cl in the atmosphere, Ber. Bunsenges. Phys. Chem., 96, 488–493, 1992.